Correlation between structural aspects and mechanical properties of an Interstitial Free steel for automotive application

Mykhaylo Romanyuk[1], Martina Avalos[2], Edgardo R. Benavidez[1] and Elena Brandaleze[1]*

[1]*Process Technology: Metallurgy Department, DEYTEMA Centre, Universidad Tecnológica Nacional-Facultad Regional San Nicolás, Colón 332, San Nicolás, 2900, Argentina.*
[2]*IFIR-Conicet, Universidad Nacional de Rosario, Ocampo y Esmeralda, Ocampo 210 bis, 2000, Rosario, Argentina.*

*Corresponding author

DOI: 10.5185/amp.2018/916
www.vbripress.com/amp

Abstract

The application of IF steels in the automotive industry has increased significantly due to their excellent deep drawability. The chemical composition, the microstructure, the precipitation phenomena and texture of the material determine the mechanical properties. This paper proposes, a more profound study of some aspects related to the application of high plastic deformation, as well as its relation with the formation of fine grain structures, texture, precipitates and grain boundaries interaction. The structure of an IF steel plate with ultra-low carbon was characterized using optical microscopy and scanning electron microscopy (SEM). A ferritic structure with very fine and recrystallized grains containing high number of triple point was observed. The precipitation kinetic of the steel was simulated applying Fact Sage 7.1. The main precipitates predicted are: TiN and TiS, these types of second phases improve the drawability behaviour. The formability aptitude of the sheet was evaluated by different mechanical tests: Hole Expansion, Erichsen and n-r determination. Finally, yield strength, tensile strength, percentage elongation and average r-value results, are correlated with the structural information. A strong (111) <110> recrystallization texture confirms the high formability of the IF steel sheet.

Keywords: Interstitial free, deep drawing, microtexture, precipitates.

Introduction

Steel has become an integral part of life in industrially developed countries; it is evident when observing the development of the automotive industry [**1**]. Currently the main objective is to reduce the weight of body and outer car panels while maintaining strength, formability and dent resistance. However, conventional high strength steel sheets have insufficient formability to satisfy the current drawing requirements of complex car panels. To predict, understand and control the mechanical behaviour constitute the most important task when designing structural materials. In recent years low and ultra-low carbon steels like extra deep drawing aluminum killed, interstitial free, interstitial free high strength and bake hardening steels have attracted attention for their formability and for this reason they are extensively used for auto bodies [**2-4**]. In metal forming, interstitial free (IF) sheets usually suffer large plastic deformation and develop nonuniform stress-strain fields [**5**].

In the majority of the nanostructures alloy systems, ductility is limited because of lack of strain hardening ability. For this reason, improvement in plasticity continuous to be the subject of interest. Particularly in the ultra-low carbon steels, called interstitial free (IF), whose application in the automotive industry has increased significantly in the last couple of decades due to their excellent deep drawability aptitude. In addition, requirements of IF steels also involve high resistance (particularly outer body car panels). This feature is achieved through chemical composition, controlled process conditions and the development of an adequate microstructure through rolling processes. The main objective is to achieve a fine grain size and a suitable precipitation [**2-7**]. In this paper, it is proposed a more profound study of some aspects related to the application of high plastic deformation, as well as its relation with the formation of fine grain structures, precipitates, texture and grain boundaries interaction; where the kinetics of precipitation as a function of temperature plays a very important role. In this sense, the study of ultrafine grain materials (UFG) is relevant and grain boundary sliding is the most important mechanisms of plasticity involved. Grain boundaries (GBs) play a fundamental role in those steels in which the mechanical properties depends on grain size. Fine grain size is preferred because the number

of grain boundaries involved in sliding is high and the distance for accommodation by diffusion and/or slip is small. Ultra-fine grain size (UFG) steels are processed by severe "cold drawing" deformation followed by annealing heat treatment. It is important for the steel to possess high thermal stability in order to retain its fine microstructure and to provide outstanding mechanical properties in the final product. The precipitation phenomenon controls the recrystallization, the final ferrite grain size and the texture. Zheng *et al.* propose that the strong {111} recrystallization textures, are beneficial to achieve a deep-drawing aptitude [**8**].

A fine dispersion of particles (nanoprecipites) in the austenite grain boundaries at processing temperatures, results in fine (austenite) grain size, which promotes ultrafine ferritic grain size in the steel during cooling at room temperature. Ti, Nb and V or a combination of these are added to ULC steels in order to capture the carbon, control the final ferrite grain size and texture. Gosh *et al.* have studied the thermodynamics aspects of precipitation and texture development in ULC steels. Different carbides, nitrides and carbonitrides are formed. The work hardening or dislocation strengthening mechanisms can result in very high levels of strength in steels with ultra-low carbon content [**3-9**].

The main novelty introduced by this paper is the discussion about strength, ductility and strain capacity values dependence with the deformation mechanisms at nanoscale. In addition, it is important to evaluate the impact of the precipitation phenomenon on the mechanical properties. The precipitation kinetic is predicted by thermodynamic simulation applying FactSage taking into account industrial process conditions [**10**]. This information is of great interest to the steel industry whose challenge is to contribute to the automotive industry in the production of safer cars to preserve human life and decrease the weight in order to have a favorable impact on fuel consumption.

Experimental

Material

The selected material for this study is an IF steel sheet with a thickness of 0.8 mm. The chemical composition is detailed in (**Table 1**).

Table 1. Chemical composition of the IF steel in weight %.

C	Ti	V	N	S	Mn	P	Cr	Si
0.0015	0.051	0.003	0.0047	0.0011	0.095	0.018	0.009	0.009

Characterization

The structural study of the IF steel sheet (as received) was carried out applying the optical microscope Olympus GX51 with an image analyzer Leco IA32. Samples were included with high-density phenolic resin and prepared by mechanically polished with 180 µm to 1200 µm SiC papers. The final polishing was carried out by 6 µm, 3 µm and 1 µm diamond paste. The metallographic etching used was a solution of (2 %) Nital. Scanning electron microscopy (SEM) studies were conducted with a FEI Quanta 200 F microscope. Besides, energy dispersive spectrometry (EDS) was applied to analyse the precipitates. Microscopic texture was determined using electron backscatter diffraction (EBSD) and the OIM software of EDAX. The precipitation kinetic of the system, was predicted through thermodynamic simulation carried out by FactSage 7.1., applying the FSteel and Misc databases. The simulations considered the chemical composition of the steel, in order to predict the precipitates formation within the structure, at temperatures between 350°C and 1150°C. The mechanical behavior of the metal sheet is evaluated by means of different mechanical tests to establish the capacity of material formability. Erichsen and Hole Expansion tests were performed by an Erichsen CIFIC machine. Erichsen measurements were obtained from an average of 3 tests, determining an Erichsen Index (EI) for a 2 tons load (corresponding to the depth of the cup). For the Hole Expansion test the obtained results correspond to a 10 tons load, that is the maximum permissible value for the machine. The result is expressed as λ value, given according to equation (**1**), where D_I is the initial diameter (10 mm) and D_F is the final diameter. The λ value is determined on the base of the average of 3 measurements.

$$\lambda = \frac{D_F - D_I}{D_I} \times 100\ (\%) \qquad (1)$$

The n–r determination was carried out by an INSTRON 4486 testing machine, with a load limit of 30 tons. These results are correlated with those obtained on the microstructure, texture, thermal behaviour and precipitation kinetic of the IF steel.

Results and discussion

Microstructure and thermodynamic simulation

The microstructure observed by optical microscopy reveal essentially the presence of fully ferritic structure **Fig. 1**, with very fine grain size (average value ASTM 14) and equiaxed shape, as a result of the recrystallization produced during steel annealing. **Fig. 1 (a).** Some grain boundaries are more prominent than others. According to Ooi et al. [**2**] three types of grains are identified in IF steel sheets depending on the morphological characteristics during etching: α grains, γ grains and {110}<110> oriented grains. The first type (α grains) is lightly etched and the second type (γ grains) is more strongly etched, see **Fig.1 (b).**

Besides, the presence of very fine precipitates is observed both inside the ferrite grains and in grain boundaries. Grain boundaries are considerable straight and there is an important presence of triple points, indicating that the material is well stabilized and recrystallized, justifying its high ductility. The structural aspects described were corroborated by (SEM). In addition, the precipitates present in triple points, along the grain boundaries and into ferritic grains were analyzed with EDS. The precipitation process in the IF steels is

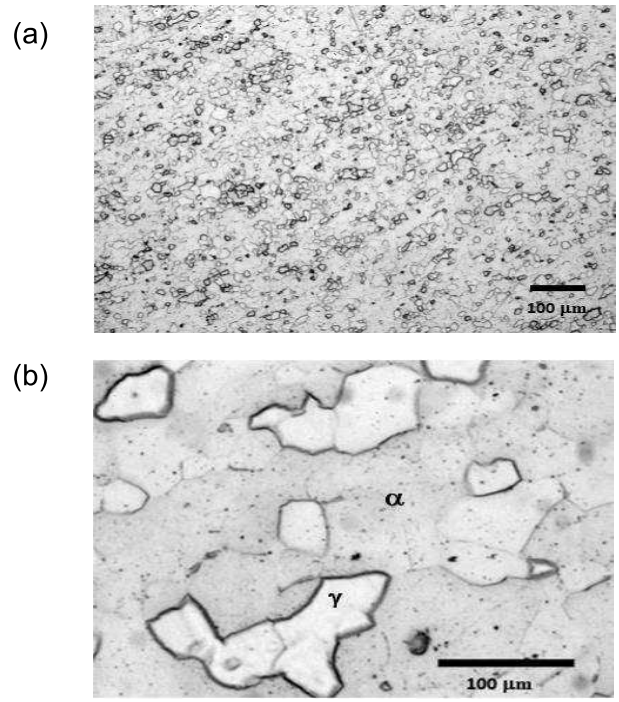

Fig. 1. (a) Ferritic structure with fine grain size, (b) Details of α and γ grains aspects and different types of precipitates present in the structure.

considered complex and its common to observe the presence of precipitates such as: TiN, TiS, TiC, $Ti_4C_2S_2$ and NbC [**2**, **11**]. In the IF sheet studied (with Ti and V content) cubic precipitates of TiC and TiN (≈ 5 µm) were identified. Furthermore, spherical TiS, TiMnS particles with an average size between 0.5 to 1 nm were also determined. It was observed that, precipitates such as TiN and TiS are randomly distributed within the ferritic matrix in coincidence with [**11**]. The precipitation of TiN and TiS instead of TiC and $Ti_4C_2S_2$ is desirable since this type of particles improve the drawability [**2, 8, 14**]. The presence of few Ti_3AlC precipitates was visualized in the structure. This type of precipitates are considered detrimental since they are usually coarse and could affect the bake hardening. According to Zheng *et al.* [**8**], the content of P in the steel could generate FeTiP particles. The authors mentioned that P accumulates at the bottom of the edge dislocation since the radius of P (0.109 nm) is smaller than that of α Fe (0.124 nm). After batch annealing, the size of FeTiP precipitates is big and present high content of P. On the contrary, after the continuous annealing process, the FeTiP is nucleated on the pre-existing TiC and the content of P is low [**8, 15**]. On this base, in the IF sample studied it is possible to consider that the FeTiP precipitates identified are nucleated on TiC precipitates, because they present low content of P, see **Fig. 2**.

It is possible to think that the P segregated in the grain boundaries, interacts with Ti and Fe atoms to form this type of precipitate. Previous studies have shown that the formation of FeTiP particles strongly affects the formation of {111} recrystallization texture, which is beneficial for deep drawing properties [**8-15**].

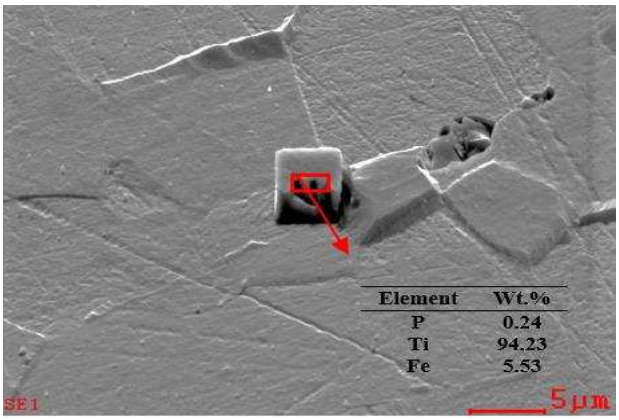

Fig. 2. FeTiP precipitates identified in the ferritic grain boundaries.

Through thermodynamic simulation using FactSage 7.1 and considering the steel chemical composition and temperatures between 350ºC to 1150ºC, the stable precipitates were determined. In agreement with Ooi *et al.*[**2**], it is assumed that the entire content of C, N and S is stabilized by the Ti, V and Mn contents in the IF steel. In coincidence with [**2, 8, 9, 13**], the results confirm that the main precipitates that can be found in the steel at the mentioned conditions are: TiN, $C_2S_2Ti_4$ and TiC. **Fig. 3.**

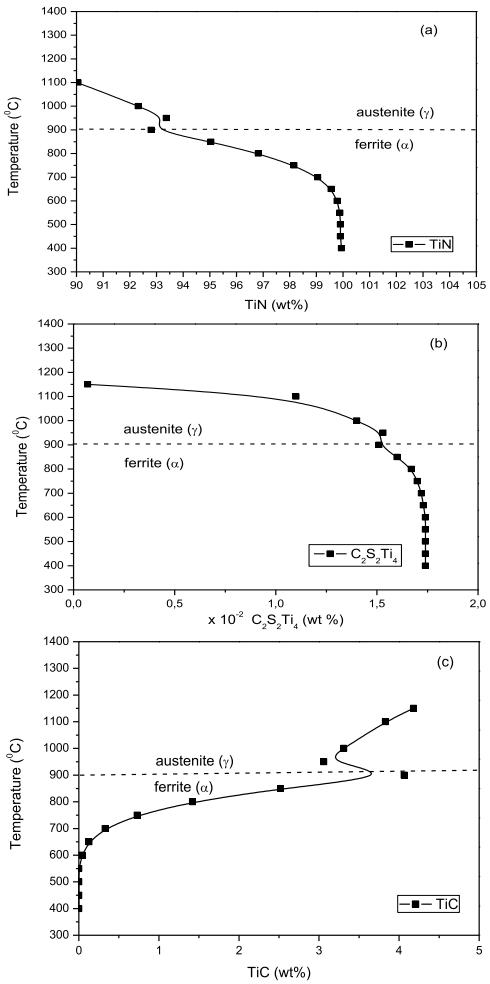

Fig. 3. Precipitation curves as a function of temperature from 1150ºC (a) TiN curve, (b) $C_2S_2Ti_4$ curve, (c) TiC curve.

The TiS precipitates observed by SEM are stable at temperatures higher than ≥1100ºC. It is observed that TiN and $C_2S_2Ti_4$ amounts increase in the steel during cooling conditions from 1150ºC, see **Fig 3(a)** and **Fig 3(b)**. The thermodynamic simulation predicts that the percentage of TiN precipitate formed in the IF steel could be greater than $C_2S_2Ti_4$. It is relevant to comment that the percentage of each precipitate (wt %) is quantified in relation to the 100% of the total volume fraction of precipitates predicted for the IF steel. Both precipitates are stable in austenite (γ) structure; however, the volume fraction shows a considerable increase in the ferrite (α) phase. This result justifies the main impact of TiN in the texture evolution and ferrite final grain size control. The small amount (Mn, Fe)S precipitation in ferrite (α) phase is due to the presence of large amounts of Ti added to the steel. The greater volume fraction of TiN and the low content of TiS are beneficial for the formability of the steel. On the contrary, TiC and $C_2S_2Ti_4$ formation is detrimental because they decrease the drawability of the material. $C_2S_2Ti_4$ precipitate will surround the TiS particles [**2, 8, 9, 13**]. The TiC and VC decreases as the annealing temperature increases, especially evident at 700ºC. Ooi *et al.* propose that the precipitation of VC is enhanced when the cooling rate from the coiling temperature is very low. The V(C, N) in ferrite could co-precipitate on preexistent TiN particles [**2**]. MnS could occur at temperatures around 1200ºC; however, the formation in this case is negligible. This precipitate is also undesirable because it generates S reduction, providing greater space for the C at the grain boundaries [**2, 8**].

Texture effect

The structural characterization is correlated with the bulk texture results measured by X ray diffraction and the information obtained from EBSD data. The strong γ–fibre {ND//<111>} recrystallization texture, measured by XRD in the IF steel, is beneficial for deep drawing property. This information is consistent with the (γ grains) visualized more strongly etched by OM and SEM. In addition, a proportion of α–fibre {<110>//RD} is detected. The structural study also verifies the presence of (α grains) that are observed lightly etched. **Fig. 4,** shows the inverse pole figure obtained from data collected by EBSD scans applying OIM. A maximum in the {111} component was determined. The result allows to think in good formability aptitude of the IF sheet. The α–fibre could be considered harmful for deep-drawing properties of the sheet. The proportion of α–fibre presence in the structure, is controlled by the oriented nucleation process [**8**]. In general, nucleation during recrystallization can occur by strain induced boundary migration (SIBM) or by subgrains growth. The driving force for SIBM is the difference in the stored energy between two neighboring regions/grains across a high angle boundary (> 15º misorientations) created during deformation. In this material, it was possible to establish misorientations angle distribution up to 60º. The highest number fraction of low angle misorientations is obtained for values < 5º. On the contrary, the highest number fraction of the high angle misorientations is observed for 60º.

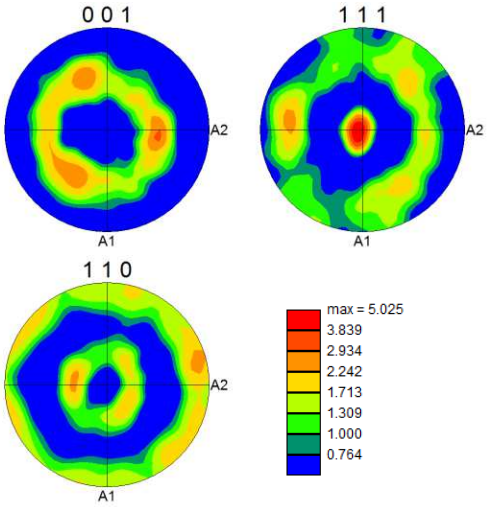

Fig. 4. Inverse pole figures obtained by EBSD on the IF steel sheet.

The (IPF) maps corroborate the misorientations of the grains associated with the microtexture. The grain map shows grain boundaries with high angle misorientations in black and grain boundaries with low angle misorientations in red. **Fig. 5.**

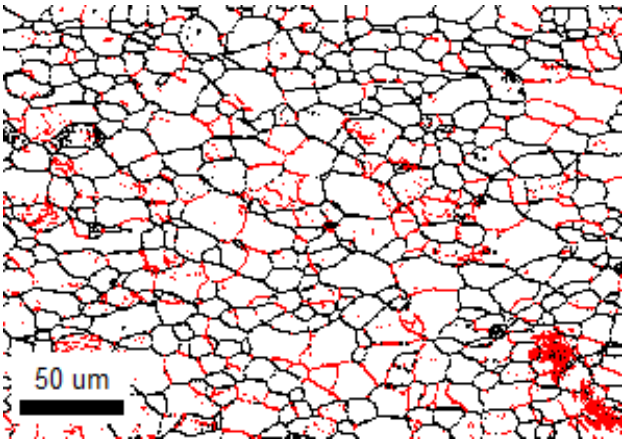

Fig. 5. Grain map showing (a) high angle misorientations grain boundaries in black, (b) low angle misorientations grain boundaries in red.

Also, the subgrains presence manifests itself through a change of color within the same grain in the IPF maps. According to Li *et al.* [**16**], materials with a gradient design, in which the grain size spans over four orders of magnitude can make strong nanomaterials ductile. The enhance ductility is attributed to the considerable strain hardening capability obtained in gradient metals. Their formation mechanisms and texture evolution have been studied profoundly in the literature. In addition, the crystal rotation path during rolling and the impact of alloying elements and second phase particles on texture formation have been studied by different authors [**8, 17**].

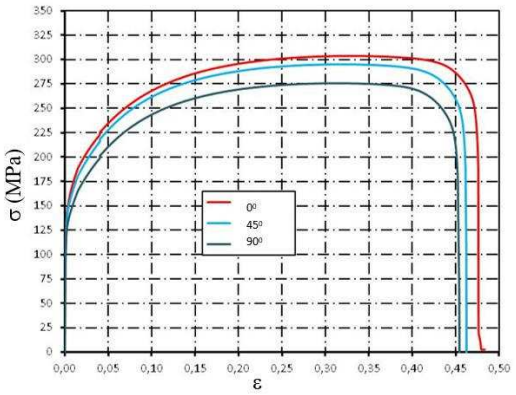

Fig. 6. Tensile test curves performed (a) Sample L1 at 0º respect RD, (b) Sample D1 at 45º respect RD and (c) Sample T1 at 90º respect RD.

Mechanical properties

The deep drawability of the IF sheet was evaluated through different mechanical tests. Through the Erichsen test results, it was possible to determine that the sheet present a good mechanical property due to the Erichsen index (IE) value of 12.7 mm. Furthermore, the samples present a normal fracture surface. Hole Expansion test results, according to equation (**1**), corroborate the drawability aptitude through the λ value (132 %). It is important to highlight that λ value of the sheet could be also higher if it is measured with a test machine with greater load limit. Both results corroborate a great mechanical response of this IF material. **Fig. 6**, shows tensile test curves performed on samples considering 0° (L1), 45° (D1) and 90° (T1) as regards the rolling direction (RD). A similar behavior between the three curves is determined. The greatest deformation capacity was obtained for 0° (L1) sample (coincident with the RD direction).

One of the most relevant requirements for a steel sheet to be suitable for extra deep drawing is to have a high normal plastic anisotropy coefficient (r) and low planar anisotropy coefficient (Δr) [**3**]. Therefore to maximize r and minimize Δr the ideal crystallographic texture for deep drawing are the components {111} <112> and {111} <110> of the γ-fibre, because this texture generates an adequate sliding systems orientation. The affirmation is consistent with the structural observations, texture measurements and the precipitates determined. On this base, the resistance in the thickness direction is greater than the resistance in the plane of the sheet [**6**]. The Δr values obtained are appropriates ($\Delta r \approx 0.17$), adjusting in both cases to the requirements of aptitude for the extra deep drawing [**6**]. The r_m coefficient values obtained are 1.92 and 1.91; both above the minimum of 1.8 required for good drawability (established by the norm) [**17**]. Analyzing the hardening coefficient (n), all values obtained are above 0.220, which is established as the minimum value according to [**6**]. On the mechanical behaviour the IF steel sheet studied is suitable for extra deep drawing. The information obtained is consistent with values informed by some authors [**7, 17**], achieving a correct stretching without producing material's necking. (**Table 2**) summarizes the results of the coefficients obtained.

Table 2. Normal (r) and average (r_m) plastic anisotropy coefficient (r), planar anisotropy coefficient (Δr), hardening coefficient for IF steel.

Sample	r	r_m	Δr	n
0º	1.93	1.92	0.17	0.260
45º	1.84			0.253
90º	2.09			0.255

On the results obtained in this paper is evident that in IF steels, both the texture and the chemical composition represent critic aspects to control the strength. The chemical composition promote the reduction of solute carbon and nitrogen and it is often compensated by addition of solid solution strengthening elements like P, Mn and Si. Si affects the coating adhesion. Mn addition reduce the normal anisotropy and total elongation. P increase the strength without causing loss in deep drawability [**18**]. In this IF steel, the contents of Mn (0.095 wt%) and P (0.018%) are considered acceptable due to the good drawability achieved. However, to produce high strength and high ductility steels, it is necessary to conduct further research in order to understand the fundamentals of gradient nanostructured metals that can achieve a good balance of both mentioned properties. According to Li *et al.*, it is relevant to increase the knowledge on the non-uniform deformation that might generate geometrically necessary dislocations (GNDs) into a gradient nanostructured steels and their effects on strength and ductility behaviour [**16**].

Conclusion

The characterization of the IF steel sheet with very low carbon content (0.0015 wt%) and Ti-V as microalloy elements, verifies that the structure is a completely recrystallized ferritic one, with very fine grain size (ASTM - G=14). Through optical microscopy and SEM the presence of γ-grains and α-grains, were identified. The results were consistent with the bulk {111} texture results obtained by X ray diffraction and the information obtained through the application of EBSD technique application that corroborates the adequate proportion of three types of grains: α fiber, γ fiber (beneficial for the extra deep drawing) and grains {110} <110>.

The structure present different types of precipitates: TiN, TiC, TiS/TiMnS and FeTiP, located randomly at the grain boundary and the interior of the grains. VC content is predicted by FactSage in very low proportion; however it is not observed in the microsctructure. The presence of precipitates with cubic morphology (TiN, TiC) and spherical morphology (TiS, TiMnS), is identified in the structure using SEM and EDS analysis. The Fact Sage thermodynamic simulation corroborates the stability of the second phases identified by microscopy and makes it

possible to verify that the main precipitate is TiN, which controls the ferritic grain size and texture. The precipitate is beneficial to achieve good forming properties. Other precipitates that favor forming properties are TiS and TiMnS, but they are present in the structure in low proportion. On the other hand, the precipitates that are detrimental of forming aptitudes are TiC and FeTiP. Despite the presence of these precipitates in the structure, the volumetric fraction in which they are present doesn´t affect the mechanical behavior of drawability verified with the good results obtained by mechanical tests.

The mechanical tests are in line with those expected for a material suitable for extra deep drawing, showing an outstanding aptitude for automotive parts applications. The results of tensile, Erichsen and Hole Expansion tests verify the excellent properties for the IF steel sheet forming. The values of n and r coefficients also verify the great formability of IF steel and are consistent with the structural information, the bulk texture and crystallographic texture results obtained.

Acknowledgements

The authors gratefully acknowledges the financial support received by the Universidad Tecnológica Nacional. The authors also thank Dr. R. Bolmaro at IFIR CONICET for helpful discussions on the texture and deformation mechanisms.

References

1. Di Schino, A.; Di Nunzio, P.E.; Cabrera, J.M.; *Advanced Materials Letters*, **2017**, 8, 5, 641. **DOI:** 10.5185/amlett.2017.1487
2. Ooi, S.W.; Fourlaris, G.; *Mat. Characterization*, **2006**, 56, 214. **DOI:** 10.1016/matchat.2005.11.010
3. Banerjee, K.; Physical Metallurgy and Drawability of Extra Deep Drawing and Interstitial Free Steels, In Recrystallization; Sztwiertnia, K.; InTech, Croatia, **2016**, pp. 137-178. **DOI:** 10.5772/35073
4. Hoile, S.; *Mat. Sci. and Tech.,* **2013**, 16, 1079. **DOI:** 10.1179/026708300101506902
5. Zhang, J.; Zhou, C.L.; Li, H.B.; Zhang, X.C.; Li, M.; *JOM,* **2017**, 69, 937. **DOI:** 10.1007/s11837-017-2342-6
6. Glebovsky, V.; Crystal Growth: Substructure and Recrystallization, In Recrystallization; Sztwiertnia, K.; InTech, Croatia, **2016**, pp. 59-86. **DOI:** 10.5772/35073
7. Ushioda, K.; Yoshinaga, N.; Akisue, O.; *ISIJ International*, **1994**, 34, 1, 85. **DOI:** isijinternational1989/34/1/34.1.85
8. Zheng, R.; Song, R.; Fan, W.; *J. of Alloy and Comp.*; **2017**, 692, 503. **DOI:** 10.1016/j.jallcom.2016.09.018
9. Ghosh, P.; Bhattacharya B.; Ray, R.K.; *Scripta Mat*., **2007**, 56, 657. **DOI:** 10.1016/j.scriptamat.2006.12.044
10. Bale, C. W.; Bélisle, E.; Chartrand, P.; Degterov, S. A.; Eriksson G.; Gheribi, A.E.; Hack, K.; Jung, H.J.; Kang, Y.B.; Melançon, J.; Pelton, A.D.; Petersen, S.; Robelin, C.; Sangster, J.; Spencer, P.; Van Ende, M.A.; *Calphad*, **2016**, 54, 35. **DOI:** 10.1016/j.calphad.2016.05.002
11. Bratberg, J.; Ågren, J.; Frisk, K.; *Mat. Scie. and Tech*., **2008**, 24, 6, 695. **DOI:** 10.1179/174328407X240954
12. Hua, M.; Garcia, C.I.; Eloot, K.; DeArdo, A.J.; *ISIJ International*, **1997**, 37, 11, 1129. **DOI:** isijinternational1989/37/11/37.11.1129
13. Ghosh, P.; Ghosh, C.; Ray, R. K.; *ISIJ International*, **2009**, 49, 11, 1080. **DOI:** isijinternational/49/7/49.7.1080
14. Guerenu, A. M. D.; Arizti, F.; Fuentes, M. D.; Gutierrez, I.; *Acta Materialia*, **2004**, 52, 3657. **DOI:** 10.1016/j.actamat.2004.04.019
15. Guiquin, F.; Duo, J.; Miaoyong, Z.; *Journal of Engineering Science and Technology Review*, **2015**, 8, 4, 43. **DOI:** 1791-2377/jestr.2015.08.47
16. Li, J.; Weng, G.J.; Chen, S.; Wu, X., *International Journal of Plasticity*, **2017**, 88, 89. **DOI:** 10.1016/j.ijplas.2016.10.003
17. Euronorm 10130; *In Cold rolled low carbon steel flat products for cold forming- Technical delivery conditions,* **2006.** **DOI:** labmix24.com/files/info/12039
18. Unnikrishnan, R.; Kumar, A.; Khatirkar, R.K.; Shekhawat, S.K.; Materials Chemistry and Physics, 2016, 183, 339. **DOI:** 10.1016/matchemphys.2016.08.037

